The following publication W. Qiu et al., "A Delayed-Excitation Data Acquisition Method for High-Frequency Ultrasound Imaging," in IEEE Transactions on Biomedical Engineering, vol. 65, no. 1, pp. 15-20, Jan. 2018 is available at https://doi.org/10.1109/TBME.2017.2687948.

A delayed-excitation data acquisition method for high-frequency ultrasound imaging

Weibao Qiu, Jingjing Xia, Yulong Shi, Peitian Mu, Xingying Wang, Mengdi Gao, Congzhi Wang, Yang Xiao, Ge Yang, Jihong Liu, Lei Sun, Hairong Zheng

***Abstract*—High-frequency ultrasound imaging (at >20 MHz) has gained widespread attention due to its high spatial resolution being useful for basic cardiovascular and cancer research involving small animals. The sampling rate of the analog-to-digital converter in a high-frequency ultrasound system usually needs to be higher than 120 MHz in order to satisfy the Nyquist sampling-rate requirement. However, the sampling rate is typically within the range of 40–60 MHz in a traditional ultrasound system, and so we propose a delayed-excitation method for performing high-frequency ultrasound imaging with a traditional data acquisition scheme. In this method, the transmitted pulse is delayed by a certain time period so that the ultrasound echo data are aligned into high-sampling-rate slots. Wire and tissue-mimicking phantoms were imaged to evaluate the performance of the proposed method, while a porcine small-intestine specimen and an excised rabbit eyeball were used for *in vitro* imaging evaluations. The test results demonstrate that the proposed method allows high-frequency ultrasound imaging to be implemented using a traditional ultrasound sampling system.**

***Index Terms*—High-frequency ultrasound, Imaging system, Delayed excitation, Emulated sampling rate, Compatible system.**

I. Introduction

Basic cardiovascular and cancer research has been greatly advanced by small-animal studies utilizing well-characterized models of human diseases [1, 2]. The use of high-frequency ultrasound imaging has had a profound impact on preclinical small-animal studies due to its ability to produce images with high spatial resolutions (on the order of tens of microns) at high temporal resolutions (frame rates of hundreds of images per second) [3–5]. This has enabled new methods for treating atherosclerosis [6], drug delivery, and treating tumor [7, 8] by visualizing morphology and the hemodynamics of the microcirculation. In addition, high-frequency ultrasound imaging is an established method that provides high-resolution intravascular images of the vessel wall and atherosclerotic plaques (~60 μm and ~120 μm in the axial and lateral directions, respectively) [9]. Recent studies have shown that increasing the ultrasound frequency to more than 100 MHz could enable the spatial resolution of ultrasound measurements to approach that of optical imaging methods [10, 11].

An analog-to-digital converter (ADC) is used to acquire data in a clinical ultrasound imaging system, with the sampling rate usually being within the range of 40–60 MHz in a system that acquires ultrasound echo data with a center frequency of 2–12 MHz [12]. However, the center frequency of a high-frequency ultrasound system is higher than 20-MHz [2–4], which is not compatible with traditional ultrasound scanners. A high-sampling-rate ADC needs to be used (usually operating at higher than 120 MHz) to satisfy the Nyquist sampling-rate requirement, which therefore means that traditional ultrasound systems cannot be used in high-frequency ultrasound applications. It would be hugely beneficial if a method was developed that enables a traditional scanner to be used in high-frequency ultrasound applications.

Interleaved sampling involves combining more than one ADC to increase the effective sampling rate [13, 14]. However, the need to synchronize the clocks of multiple ADCs greatly increases the complexity of the data acquisition circuits. A two-clock sampling scheme was proposed that increases the effective sampling rate by a factor of 20 or more above the basic sampling rate of the ADC, while the signal-to-noise ratio was also improved by averaging the data [15, 16]. However, this method requires two clock sources, which usually are not available in a clinical ultrasound system.

This paper presents a delayed-excitation method that allows a traditional ultrasound scanner to perform high-frequency ultrasound imaging. An imaging platform was employed for pulse generation and image processing. The sampling rate of the ADC was set to 40 MHz or 80 MHz, which is compatible with traditional scanners. The emulated sampling rate was 160 MHz for acquiring data at a high ultrasound center frequency (40 MHz). A single-element focused ultrasound transducer was

Manuscript received Jul 15, 2016. This work was supported by the National Science Foundation Grants of China (61302038, 81527901, 61571431, 11325420, and 11534013), National Basic Research Program of China (2015CB755500), CAS research projects (Y650311C31, and QYZDB-SSW-JSC018), Guangdong Innovative and Entrepreneurial Research Team Program (2013S046), Natural Science Foundation of Guangdong Province (2015A030306018, 2014A030313686 and 2014A030312006), Shenzhen Peacock Plan (20130409162728468), Shenzhen International Collaboration Grant (GJHZ20140417113430615), and Shenzhen Foundation Grant (JCYJ20140610151856707).

W. Qiu*, J. Xia, Y. Shi, P. Mu, X. Wang, C. Wang, Y. Xiao, G. Yang, L. Sun, J. Liu and H. Zheng* are with the Institute of Biomedical and Health Engineering, Shenzhen Institutes of Advanced Technology, Chinese Academy of Sciences, Shenzhen 518055, China (corresponding author, e-mail: wb.qiu@siat.ac.cn, hr.zheng@siat.ac.cn).

Y. Shi, M. Gao, and J. Liu are with the Sino-Dutch Biomedical and Information Engineering School, Northeastern University, Shenyang 110169, China.

L. Sun is with the Interdisciplinary Division of Biomedical Engineering, The Hong Kong Polytechnic University, Hong Kong, China.

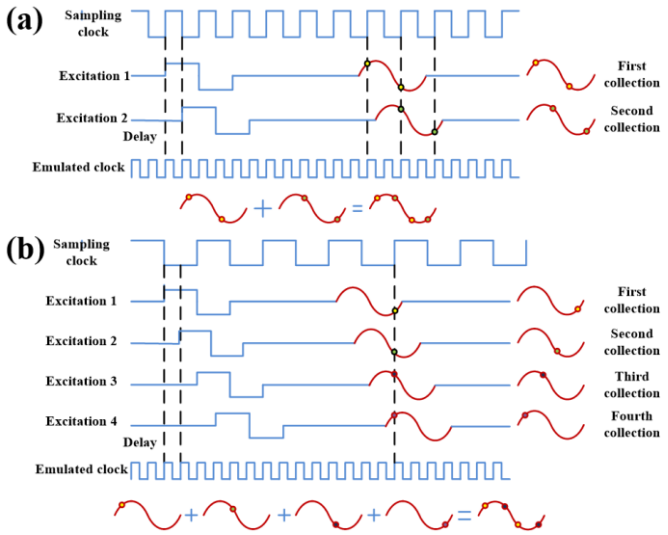

Fig. 1. Principle of the delayed-excitation imaging methodology with different ADC sampling rates. (a) Emulated sampling rate that is two times higher than the sampling rate of the ADC implemented using a half-cycle pulse delay. (b) Emulated sampling rate that is four times higher than the sampling rate of the ADC implemented using a quarter-cycle pulse delay.

used to evaluate the imaging performance. A wire phantom, tissue-mimicking phantom, and *in vitro* tissue were imaged to demonstrate the performance of the proposed method.

II. Methods

A. Delayed Excitation Method

Fig. 1 presents the principle of the delayed-excitation method. The sampling clock shown in the figure is the sampling rate of the ADC in a traditional ultrasound scanner. The Nyquist sampling-rate requirement is not satisfied since the sampling rate is not at least twice the ultrasound frequency. Fig. 1(a) shows that two excitations are used to compose one sequence of echo data. The second excitation pulse is delayed by half a cycle, which results in a different sampling position for the ultrasound echo data. The echo signal is acquired at four different positions over one full clock cycle by two-times delayed-excitation data acquisition, so that the emulated high-frequency clock is two times higher than the ADC clock. Similarly, the emulated sampling rate is four times higher than the ADC clock when the delay was set to one-quarter of the ADC clock, resulting in four-times pulse excitation and data acquisition (shown in Fig. 1(b)).

The Field II program was first used for wire-phantom simulation. Fig. 2 shows that eight points were defined in the *x*-*z* plane with a lateral separation of 1 mm and an axial separation of 0.5 mm. The center frequency of the single-element transducer was set to 35 MHz and the focal depth was 7 mm. All of the images are displayed with a dynamic range of 45 dB. The simulation results show noticeable distortions in the axial direction for both the 40 MHz and 80 MHz ADCs where the echo signal was fully recovered using the proposed two-times delayed-excitation data acquisition method.

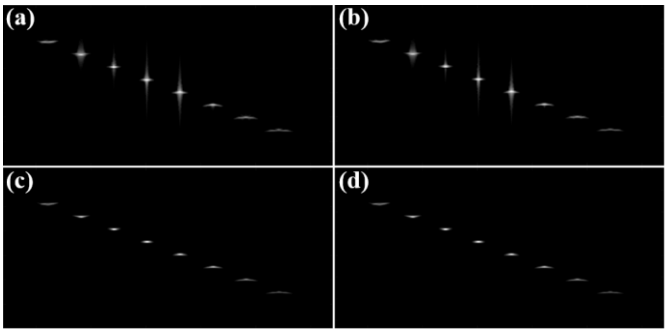

Fig. 2. Results from Field II simulations of the wire phantom. (a) Image acquired using the 40 MHz ADC. (b) Image acquired using the 80 MHz ADC. (c) Combined image obtained using the two-times delayed-excitation method. (d) Image acquired using the 160 MHz ADC. Dynamic range of 45 dB.

B. Imaging Platform

A high-frequency ultrasound imaging platform was used to evaluate the imaging performance of the proposed method [17]. A metal-oxide-semiconductor field-effect transistor (MOSFET) (TC6320, Supertex, Sunnyvale, CA) was used to generate a bipolar pulse with an amplitude of ±48 Vpp. A low-noise amplifier (AD8331, Analog Devices, Canton, MA) was used as the echo signal amplifier. To allow a fair comparison, another ADC (AD9230, Analog Devices) was operated at 160 MHz throughout the experiments. Down-sampling was employed by extracting two-times and four-times delayed-excitation data for sampling rates of 80 MHz and 40 MHz, respectively. A field-programmable gate array (FPGA) (Cyclone-V 5CGXFC7D7F31C8N, Altera Corporation, San Jose, CA) was employed to implement data acquisition and the user interface. In addition, a clock generator (CDCM61002, Texas Instruments, Dallas, TX) served as a clock source, and DDR3 SDRAM (MT41J128M16HA, Micron Technology, Boise, ID) was used for data buffering. The raw radiofrequency (RF) data were acquired and sent to a PC for post-processing through a USB (Universal Serial Bus) 3.0 interface (CYUSB3014, Cypress, San Jose, CA).

C. Transducer and Imaging Parameters

A press-focused ultrasound transducer [18] with an aperture size of 3.0 mm was fabricated and used in this study. The focal distance was 7 mm. A lithium-niobate single crystal (Boston Piezo-Optics, Bellingham, MA) was selected as the piezoelectric material of the transducer, and it was designed with a center frequency of 35 MHz.

The transducer was fixed onto a linear motor stage (PLS-85, PI miCos, Eschbach, Germany) to allow linear imaging scans to be performed. The motor was moved at a speed of 8 mm/s. The image was constructed using two-times delayed-excitation scanning with the 80 MHz ADC and four-times delayed-excitation scanning with the 40 MHz ADC. The emulated clock rate was 160 MHz for high-frequency data acquisition. A single-cycle bipolar pulse was generated by the imaging platform with an amplitude of ±48 Vpp. Each image comprised 600 A-lines, with each A-line contained 3072

sampling points. The pulse repetition frequency was about 305 Hz. The step size in the axial and lateral direction were about 4.8 μm and 26.2 μm respectively.

D. Phantom Fabrication and Evaluation

Two phantoms were fabricated for evaluating the imaging performance. One of them was a wire phantom consisting of eight tungsten wires with a diameter of 20 μm (California Fine Wire, Grover Beach, CA) arranged with equal spacing in the radial (0.5 mm) and lateral (1 mm) directions. The axial and lateral resolutions of the system were quantified based on the evaluations of the wire phantom.

A cylindrical agar-based tissue-mimicking phantom containing three anechoic holes was also fabricated. This phantom had tissue-mimicking attenuation and backscattering characteristics designed to test the resolution and depth of field. The three anechoic holes had diameters of 0.5 mm, 1.0 mm, and 1.5 mm, and were spaced uniformly in the phantom. The contrast-to-noise ratio (CNR) of the anechoic hole was calculated to provide an indirect characterization of the spatial resolution of the device in all three orthogonal directions simultaneously [10].

III. Results

A. Pulse-Echo Evaluation

A flat glass target was placed in front of the transducer perpendicular to the acoustic propagation beam. The echo signal was acquired by the imaging platform. Fig. 3 shows typical acquired signal waveforms and spectrums. The waveforms were distorted when using sampling rates of 40 MHz and 80 MHz without delayed excitation, as shown in Fig. 3(a–d). Fig. 3(c) shows the combined waveforms using two-times 80 MHz ADC data acquisition. This figure indicates that the combined ultrasound echo signal was fully recovered after implementing the delayed-excitation method. Fig. 3(d) shows the waveform acquired using the 160 MHz ADC. Fig. 3(e) shows data spectrums when using the two-times delayed-excitation data acquisition method and the 160 MHz ADC. The center frequencies were 32.7 MHz and 32.1 MHz, and the corresponding -6 dB bandwidths were around 56.3% and 55.6% respectively.

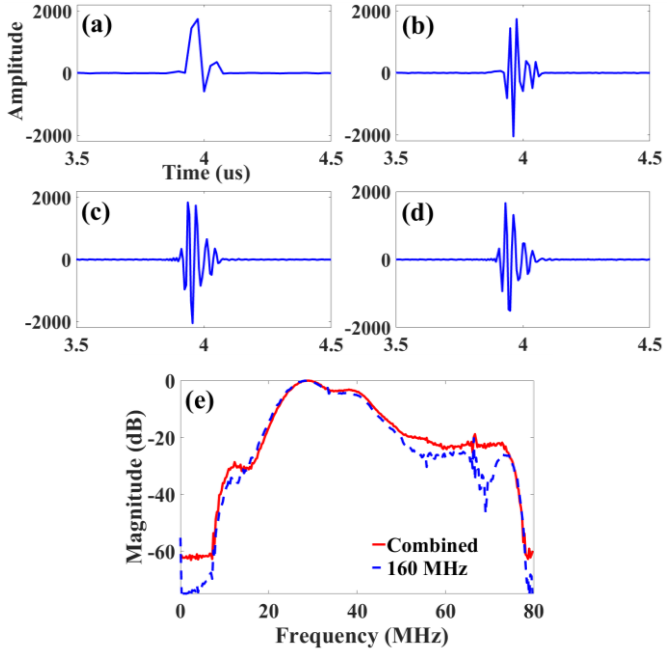

Fig. 3. Typical waveforms, and spectrums in a pulse-echo evaluation. The center frequency of the excitation pulse was 35 MHz, and the emulated clock rate was 160 MHz. (a) Waveform acquired using the 40 MHz ADC with a 6.25 ns excitation delay. (b) Waveform acquired using the 80 MHz ADC with a 12.5 ns excitation delay. (c) Waveform recovered using two-times delayed-excitation method. (d) Waveform acquired using the 160 MHz ADC. (e) Spectrums of data using the two-times delayed-excitation method (red line) and using the 160 MHz ADC (blue line).

B. Imaging of Wire Phantom

The imaging quality of the proposed device was first evaluated using the customized tungsten-wire phantom. Fig. 4 shows acquired images of the wire phantom. Noticeable distortion was evident along the axial direction (Fig. 4(a)) when 40 MHz sampling was employed. The image quality was improved when sampling at 80 MHz, but noticeable distortion was still presented (Fig. 4(b)). Employing the delayed-excitation method yields the image shown in Fig. 4(c). There is no noticeable noise in the image, and it does not differ noticeable from the image obtained by direct high-frequency sampling (Fig. 4(d)). Fig. 4(e, f) show the axial and lateral envelope data obtained when using the two-times delayed-excitation data acquisition method (red line) and the

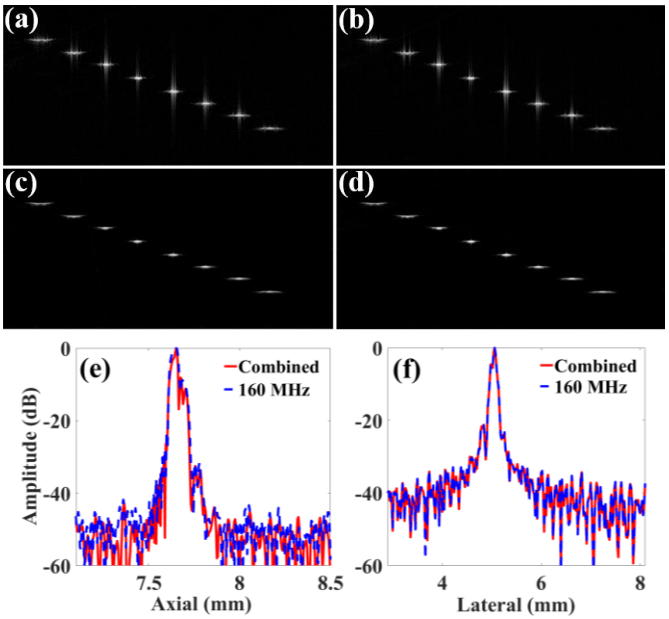

Fig. 4. Images of the wire phantom obtained using the imaging system with different sampling schemes. (a) Image acquired using the 40 MHz ADC with a 6.25 ns excitation delay. (b) Image acquired using the 80 MHz ADC with a 12.5 ns excitation delay. (c) Combined image for the two-times delayed-excitation data acquisition method. (d) Image acquired using the 160 MHz ADC. (e) Axial cross section view obtained using the two-times delayed-excitation data acquisition method (red line) and using the 160 MHz ADC (blue line). (f) Lateral cross section view obtained using the two-times delayed-excitation data acquisition method (red line) and using the 160 MHz ADC (blue line). Dynamic range of 45 dB.

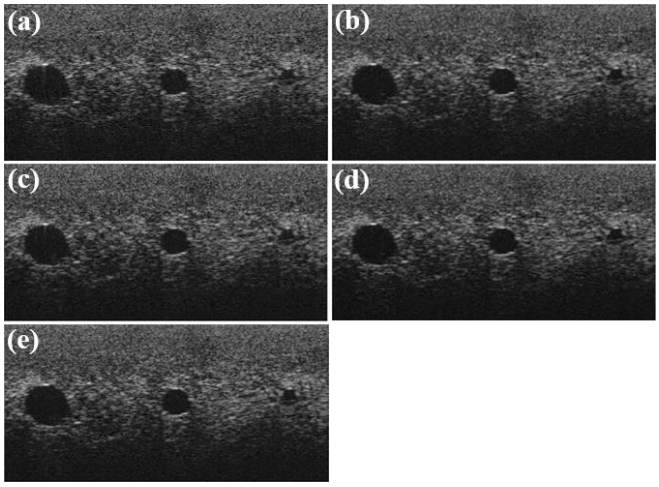

Fig. 5. Images of the tissue-mimicking phantom acquired by the imaging system with different sampling schemes. (a) Image acquired using the 40 MHz ADC. (b) Combined image for four-times delayed-excitation data acquisition. (c) Image acquired using the 80 MHz ADC. (d) Combined image for two-times delayed-excitation data acquisition. (e) Image acquired using the 160 MHz ADC. Dynamic range of 40 dB.

160 MHz ADC (blue line), for which the axial and lateral resolutions around the focal point were about 48 μm and 110 μm, respectively. The RF data used to form these images were logarithmically compressed into a 45 dB dynamic range in order to improve the image speckle pattern.

C. Imaging of Tissue-Mimicking Phantom

Fig. 5 shows ultrasound images of the tissue-mimicking phantom. There are obvious imaging errors in Fig. 5(a, c). By combining several delayed-excitation data sequences, images were recovered that were similar to those obtained with the commercial ultrasound scanner. The anechoic holes were visualized using the new system when the dynamic range was set to 40 dB. The focus was located 5 mm below the surface of the tissue-mimicking phantom. The penetration depth—defined at the place in the phantom where the signal amplitude was decreased to 6 dB—was 7 mm in Fig. 5(b). Fig. 6(a–d) are zoomed-in views of the largest holes in Fig. 5(a), (b), (c), and (d) respectively; the average CNRs in these four images were 6.9, 8.7, 9.4, and 9.6, respectively. Numerical comparisons indicate that the combined image recovered using the

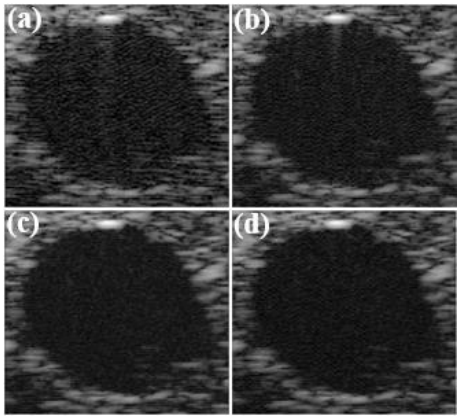

Fig. 6. Enlarged view of the left largest hole in Fig.5.(a, c, d, e). Dynamic range of 40 dB.

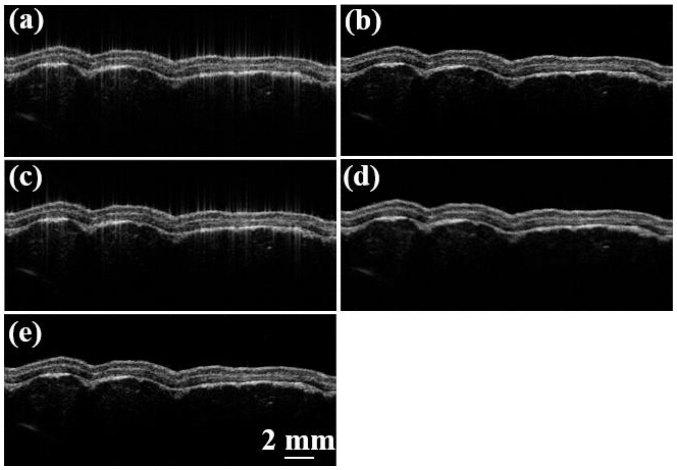

Fig. 7. Images of the porcine small-intestine specimen. (a) Image acquired using the 40 MHz ADC. (b) Combined image for four-times delayed-excitation data acquisition. (c) Image acquired using the 80 MHz ADC. (d) Combined image for two-times delayed-excitation data acquisition. (e) Image acquired using the 160 MHz ADC. Dynamic range of 45 dB.

delayed-excitation method exhibited equivalent CNRs to the image acquired using the 160 MHz ADC.

D. In vitro Measurement of Tissue Samples

A porcine small-intestine specimen was used for *in vitro* imaging evaluations. The specimen was cut into pieces and gently unfolded by a holder. The transducer was scanned over the tissue sample immersed in a water tank to obtain the cross-sectional ultrasound images shown in Fig. 7. The images were distorted due to the low sampling rate, but all could be successfully recovered by applying the delayed-excitation sampling scheme. These measurements were made with a dynamic range of 45 dB. Different layers of the lumen wall could be clearly identified when using the proposed imaging method.

An excised rabbit eyeball was also employed to evaluate the imaging performance. Fig. 8 shows images of the anterior portion of an excised rabbit eye. The performance of the delayed-excitation imaging method was similar to that obtained when imaging the small-intestine specimen. The recovered

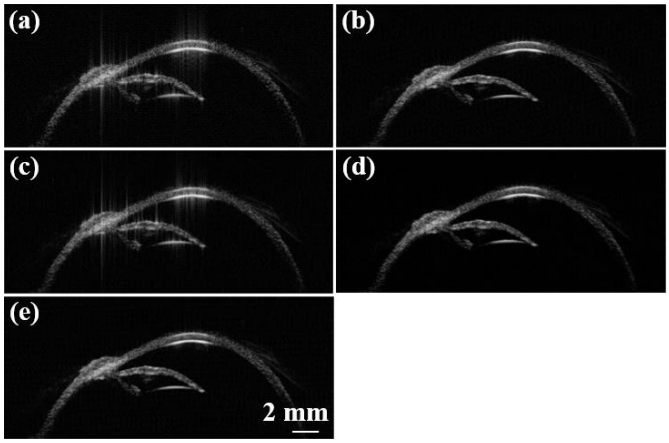

Fig. 8. Images of the excised rabbit eye. (a) Image acquired using the 40 MHz ADC. (b) Combined image for four-times delayed-excitation data acquisition. (c) Image acquired using the 80 MHz ADC. (d) Combined image for two-times delayed-excitation data acquisition. (e) Image acquired using the 160 MHz ADC. Dynamic range of 45 dB.

images appeared similar to those obtained using the commercial scanner, when the dynamic range of the images was set to 45 dB.

IV. Discussion

High-frequency ultrasound imaging is usually performed with a center frequency higher than 20 MHz, which requires the use of a high-sampling-rate ADC (usually operating at faster than 120 MHz) to satisfy the Nyquist sampling-rate requirement. However, the sampling frequency of a clinical scanner is usually within the range of 40–60 MHz, with a center frequency of 2–15 MHz. This means that the traditional ultrasound systems cannot perform high-frequency ultrasound imaging.

This paper has proposed a delayed-excitation data acquisition method for performing high-frequency ultrasound imaging using a traditional data acquisition scheme. In this study, the sampling rate of the ADC was set to 40 MHz or 80 MHz. The ultrasound echo data were aligned into high-sampling-rate slots by delaying the transmitted pulse by a certain time period (1/4, 1/2, or 3/4 cycle for the 40 MHz ADC, and 1/2 cycle for the 80 MHz ADC) ; this yielded an emulated sampling rate of 160 MHz for the data acquisition. Both wire and tissue-mimicking phantoms and *in vitro* tissues (a porcine small-intestine specimen and an excised rabbit eyeball) were imaged to evaluate the performance of the proposed method. The obtained experimental results show that the images for four-times delayed-excitation data acquisition (using the 40 MHz ADC) and two-times delayed-excitation data acquisition (using the 80 MHz ADC) were comparable to the images acquired using the 160 MHz ADC. These findings indicate that the delayed-excitation method allows high-frequency ultrasound imaging to be implemented using a traditional ultrasound sampling system.

The images acquired using the 40 MHz and 80 MHz ADCs exhibited noticeable distortions along the axial direction. These are caused by not satisfying the Nyquist sampling-rate requirement: a sampling rate lower than twice the ultrasound frequency results in some data information being lost during each sampling cycle, which leads to a wider envelope being detected after the IQ demodulation process and thereby distorts the axial waveform. Some black holes were also present around the focal region in all of the images (Fig. 5), which may have been caused by inhomogeneities in the tissue-mimicking phantom.

Since the proposed method requires multiple-times delayed-excitation data acquisition, it may not be suitable for imaging tissue that is moving rapidly. However, comparing with the pulse-inversion-based harmonic imaging method [20] reveals that multiple times delayed-excitation data acquisition would be acceptable for clinical investigations.

Components other than the ADC also need to be considered when developing an ultrasound system for use in both traditional and high-frequency ultrasound applications. Improvements in technology mean that state-of-the-art electronics now make it possible to cover a wide ultrasound frequency range of 2–50 MHz. For instance, the TC6320 MOSFET (Supertex) can be used to generate a pulse with a center frequency higher than 50 MHz [19]. Moreover, the gain bandwidth of the AD8331 amplifier (Analog Devices) is larger than 50 MHz, and highly integrated analog front-end solutions specifically designed for ultrasound imaging are available. For example, the AFE5818 device (Texas Instruments) contains 16 channels—including amplifiers, filters, and ADCs—for processing analog signals, which would facilitate the implementation of a scanner for use in a high-frequency ultrasound imaging system. It should be possible to incorporate all of the electronics in a special system both for traditional and high-frequency ultrasound imaging, given that highly integrated silicon chips have been produced, and the issue of data acquisition circuit could be solved by applying the proposed method.

The proposed method can be used to implement high-frequency ultrasound imaging using a traditional ultrasound system, but at a reduced frame rate. The travel distance in high-frequency ultrasound imaging is much less than that in a traditional scanner. For example, the travel time for a single-excitation pulse is 26 μs based on a propagation speed of 1540 m/s and a penetration depth of 20 mm. The frame rate is about 192 frames per second when using 200 A-lines to form an image, and this would decrease to 48 frames per second when applying four-times pulse excitation, but this is still fast enough for most ultrasound imaging applications.

V. Conclusion

This study has designed and tested a delayed-excitation method specifically for high-frequency ultrasound imaging. The proposed method enables traditional ultrasound scanners to perform high-frequency ultrasound imaging. The presented test results demonstrate that the traditional imaging method achieved comparable imaging performance for both phantoms and *in vitro* tissue samples, verifying that the methodology is a viable choice for fabricating a high-frequency ultrasound system.

References

[1] C. Thisse and L. I. Zon, “Organogenesis-Heart and blood formation from zebrafish point of view,” Science, vol. 295, no. 5554, pp. 457-462, 2002.
[2] F. S. Foster, et al., “Micro-ultrasound for preclinical imaging,” Interface Focus, vol. 1, pp. 576-601, 2011.
[3] J. A. Ketterling, et al., “Design and fabrication of a 40-MHz annular array transducer,” IEEE Trans. Ultrason. Ferroelectr. Freq. Control, vol. 52, no. 4, pp. 672-681, 2005.
[4] L. Sun, et al., “A high-frame rate high-frequency ultrasonic system for cardiac imaging in mice,” IEEE Trans. Ultrason. Ferroelectr. Freq. Control, vol. 54, no. 8, pp. 1648-1655, 2007.
[5] F. S. Foster, et al., “A new 15–50 MHz array-based micro-ultrasound scanner for preclinical imaging,” Ultrasound Med. Biol., vol. 35, no. 10, pp. 1700-1708, 2009.
[6] S. Mani, et al., “Decreased endogenous production of hydrogen sulfide accelerates atherosclerosis,” Circulation, vol. 127, pp. 2523-2534, 2013.
[7] S. Fokong, et al., “Image-guided, targeted and triggered drug delivery to tumors using polymer-based microbubbles,” Journal of Controlled Release, vol. 163, no. 1, pp. 75-81, 2012.

[8] A. Neesse, et al., “SPARC independent drug delivery and anti-tumour effects of nab-paclitaxel in genetically engineered mice,” Gut, vol. 63, pp. 974-983, 2014.
[9] D. Maresca, et al., “Contrast-enhanced intravascular ultrasound pulse sequences for bandwidth-limited transducers,” Ultrasound Med. Biol, vol. 39, no. 4, pp. 706-713, 2013.
[10] T. Ma, et al., “Multi-frequency intravascular ultrasound (IVUS) imaging,” IEEE Trans. Ultrason. Ferroelectr. Freq. Control, vol. 62, pp. 97-107, 2015.
[11] C. Fei, et al., “Ultrahigh frequency (100 MHz-300 MHz) ultrasonic transducers for optical resolution”, Sci. Rep. 6, 28360, 2016.
[12] W. Qiu, et al., “A scanning-mode 2D shear wave imaging (s2D-SWI) system for ultrasound elastography,” Ultrasonics, vol. 62, pp. 89-96, 2015.
[13] C. Vogel, “The impact of combined channel mismatch effects in time-interleaved ADCs,” IEEE Trans. Instrum. Meas., vol. 54, no. 1, pp. 415-427, Feb, 2005.
[14] J. Elbornsson, et al., “Analysis of mismatch effects in a randomly interleaved A/D converter system,” IEEE Trans. Circuits Syst., vol. 52, no. 3, pp. 465-476, Mar, 2005.
[15] A. N. Kalashnikov, et al., “High-accuracy data acquisition architectures for ultrasonic imaging,” IEEE Trans. Ultrason. Ferroelectr. Freq. Control, vol. 54, no. 8, pp. 1596-1605, 2007.
[16] V. G. Ivchenko, et al., “High-speed digitizing of repetitive waveforms using accurate interleaved sampling,” IEEE Trans. Instrumentation and Measurement, vol. 56, no. 4, pp. 1322-1328, August, 2007.
[17] W. Qiu, et al., “An FPGA based open platform for ultrasound biomicroscopy,” IEEE Trans. Ultrason. Ferroelectr. Freq. Control, vol. 59, no.7, pp. 1558-1567, 2012.
[18] J. M. Cannata, et al., “Design of efficient, broadband single-element (20-80MHz) ultrasonic transducers for medical imaging applications,” IEEE Trans. Ultrason. Ferroelectr. Freq. Control, vol. 50, no. 11, pp. 1548-1557, 2003.
[19] W. Qiu, et al., “A multi-functional, reconfigurable pulse generator for high frequency ultrasound imaging,” IEEE Trans. Ultrason. Ferroelectr. Freq. Control, vol. 59, no. 7, pp. 1432-1442, July, 2012.
[20] F. Tranquart, et al., "Clinical use of ultrasound tissue harmonic imaging", Ultrasound in Medicine & Biology, vol. 25, no. 6, pp. 889-894, Jul, 1999.